

Opening a closed Hamiltonian map

Miguel A. F. Sanjuán

Nonlinear Dynamics and Chaos Group, Departamento de Matemáticas y Física Aplicados y Ciencias de la Naturaleza, Universidad Rey Juan Carlos, Tulipán s/n, 28933 Móstoles, Madrid, Spain

Takehiko Horita

Department of Mathematical Engineering and Information Physics, The University of Tokyo, Tokyo 113-8656, Japan

Kazuyuki Aihara

*Department of Mathematical Engineering and Information Physics, The University of Tokyo, Tokyo 113-8656, Japan
and CREST, Japan Science and Technology Corporation (JST), 4-1-8 Hon-cho, Kawaguchi, Saitama 332-0012, Japan*

(Received 9 April 2002; accepted 22 October 2002; published 10 January 2003)

A closed Hamiltonian map is opened by introducing an interaction with the outside of the system. The resulting open Hamiltonian system possesses an exit with escaping orbits through it. For such a system equipped with two or three exits, the exit basin structure of the escaping orbits is observed to have a fractal boundary and a boundary shared by the three basins, i.e., a Wada basin boundary. In the small size limit of the exits, a complete fractalization of the phase space, where the predictability of the future state is almost lost, is also observed. © 2003 American Institute of Physics. [DOI: 10.1063/1.1528750]

The dynamics in Hamiltonian systems has been extensively investigated in many respects. For example, many researchers have paid much attention on quasiperiodic and chaotic motions in the standard map, which is an area-preserving map on a cylinder. The standard map has been mainly investigated on its property as a closed Hamiltonian system because of its discrete translational symmetry along the symmetry axis of the cylinder except on the chaotic diffusion along it. On the other hand, in open Hamiltonian systems that have escaping orbits, chaotic scattering and exit basins have been thoroughly investigated. One of the simplest examples of such open Hamiltonian systems might be a scatterer composed of hard disks. So far, in open Hamiltonian systems, there seems to be no simple system corresponding to the standard map as a closed Hamiltonian system. In the present paper, we show that a closed Hamiltonian map can be opened by introducing an interaction with the outside of the system. As a result of the interaction, the system has an exit of orbits to the outside of the system. In the phase space of such a system equipped with two or three exits, the set of the initial conditions of the orbits that escape through each of the exits is the basin of the exit. The structure of the exit basins is observed to have a fractal boundary and a boundary shared by the three basins, i.e., a boundary possessing the Wada property. With the decrease of the sizes of the exits, the fractalization of the phase space gets stronger and, in the small size limit of the exits, a complete fractalization of the phase space is also observed. In this limit, the points of different basins are uniformly mixed and the predictability of the future state is almost lost.

I. INTRODUCTION

In closed Hamiltonian systems, the Poincaré recurrence theorem states that the set of nonrecurrent points has measure zero. This statement is powerful for the future prediction in the following sense: for almost all initial states, there is an increasing infinite sequence of times at which the state gets closer and closer to the initial state as time goes, no matter how chaotic the orbit is. On the other hand, in open Hamiltonian systems, this kind of predictability might be lost as in the case of chaotic scattering.¹ Our main goal is to analyze what is observed when a closed Hamiltonian system is opened. We consider the predictability of the final state in an open Hamiltonian system. For this purpose, we open a closed Hamiltonian map by introducing an interaction with the outside of the system, where the resulting system is simply a map with an exit. By the simplicity of the system, we believe it is useful for the investigation of general properties of open Hamiltonian systems. It should be noted that open Hamiltonian systems are also important for the dynamical systems approach to transport phenomena in nonequilibrium statistical mechanics.^{2,3}

The system considered in the present paper is the standard map⁴

$$\theta_{n+1} = \theta_n + J_{n+1} \bmod 2\pi,$$

$$J_{n+1} = J_n + Kf(\theta_n), \quad (1)$$

with $f(\theta) \equiv \sin \theta$ and a constant $K > 0$, which is considered to be the Poincaré map of the kicked rotator.⁴

$$d^2\theta/dt^2 = Kf(\theta) \sum_{n=-\infty}^{\infty} \delta(t-n), \tag{2}$$

where θ is the angle variable of the rotator. Since the map Eq. (1) is invariant under the transformation $J \rightarrow J + 2\pi$, we can identify $J + 2\pi$ as J by taking modulo 2π in J . Thus the standard map Eq. (1) with modulo 2π in J composes a closed Hamiltonian system, i.e., an area-preserving map. Let us introduce an interaction with the outside of the system in the following manner: observe the angle θ of the kicked rotator at every instant just before the kicks and stop the rotator if the angle is in a given range $[\bar{\theta}_0, \bar{\theta}_1]$. Then the system is no longer closed and this procedure corresponds to introduce a stripe $[\bar{\theta}_0, \bar{\theta}_1] \times [0, 2\pi)$ on the phase space (θ, J) , which act as an exit in the sense that if the element (θ_n, J_n) of an orbit starting for (θ_0, J_0) hits the stripe for the first time at n then it is terminated. It should be noted that this is a similar idea with modifying a billiard system by opening holes.⁵

By introducing two or three exits, we observe the dependence of final states on initial states and define the “basin” of each exit.⁵ We also observe the change of “basin” structure by changing the sizes of the exits⁶ and the influence of nonhyperbolicity on the structure of the “basin.” In Sec. II, strange “basins” for open Hamiltonian maps are observed. In Sec. III, the predictability in the small size limit of the exits is considered. The last section is devoted to a conclusion.

II. STRANGE “BASINS” FOR HAMILTONIAN MAPS

The standard map with exits considered in the preceding section is expressed as

$$\begin{aligned} \theta_{n+1} &= \begin{cases} \theta_n & \text{if } (\theta_n, J_n) \in E, \\ \theta_n + J_{n+1} \bmod 2\pi & \text{otherwise,} \end{cases} \\ J_{n+1} &= \begin{cases} 0 & \text{if } (\theta_n, J_n) \in E, \\ J_n + Kf(\theta_n) \bmod 2\pi & \text{otherwise,} \end{cases} \end{aligned} \tag{3}$$

where E denotes the union of the exits. Let us consider two exits $E_1 \equiv [\bar{\theta}_0, \bar{\theta}_1] \times [0, 2\pi)$ and $E_2 \equiv [\bar{\theta}_2, \bar{\theta}_3] \times [0, 2\pi)$ and denote the set of initial points such that the orbits terminate in E_1 (E_2) as the “basin” of exit E_1 (respectively, E_2). Since $f(2\pi - \theta) = -f(\theta)$, the standard map Eq. (1) is invariant under the transformation

$$(\theta, J) \rightarrow (2\pi - \theta, 2\pi - J). \tag{4}$$

If the two exits E_1 and E_2 are symmetric with respect to the transformation Eq. (4), then the system Eq. (3) is also symmetric with respect to the transformation Eq. (4).

A. Fractal basins (two exits)

Before investigating the standard map with exits, let us consider a hyperbolic system called the sawtooth map,⁷ which is Eq. (1) with $f(\theta) = (\theta \bmod 2\pi) - \pi$ satisfying $f(2\pi - \theta) = -f(\theta)$. Since the sawtooth map has a constant Jacobian matrix

$$\begin{pmatrix} 1+K & 1 \\ K & 1 \end{pmatrix}, \tag{5}$$

its hyperbolicity is obvious for $K > 0$. The sawtooth map also has the symmetry with respect to the transformation Eq. (4) due to $f(2\pi - \theta) = -f(\theta)$.

Let us place the left exit of size w as $[0.2\pi - w\pi, 0.2\pi + w\pi] \times [0, 2\pi)$ if $0 < w < 0.2$ and $[0, 2w\pi] \times [0, 2\pi)$ if $w \geq 0.2$ and the right exit symmetrically. In Fig. 1, the basins for the sawtooth map with two symmetrical exits at $K = 0.6$ with $w = 0.3, 0.08, 0.04$, and 0.02 are shown, where the blue and red regions show the basins of the left and right exits, respectively. For the exits with small size, the basin boundary shows a fractal structure,⁸ where a small fraction of nonfractal basin boundary is also observed,⁵ such as at the boundary of exits. A transition from a nonfractal basin boundary to a fractal boundary with the decrease of exit size is also clearly observed. With the decrease of exit size, the two basins seem to be more and more mixed.

The basin boundary dimension⁸ is useful for a quantitative characterization. Let us divide the phase space into cells by covering with a grid of unit size ϵ and count the number N of the uncertain cells, each of which contains points of different basins. Figure 2(a) shows the number N of uncertain cells as a function of ϵ for various exit sizes w . The basin boundary dimension d is introduced by the relation

$$N \sim \epsilon^{-d} \tag{6}$$

for small ϵ . In Fig. 2(b), the basin boundary dimension d estimated from the log-log plot of N against ϵ in the range $2^{-12} \leq \epsilon/2\pi \leq 2^{-7}$ is shown. Note that $d = 1$ indicates a nonfractal basin boundary and the larger value of d implies the more mixed basins. The fractal structure of the basin boundary is understood by considering an invariant chaotic saddle of the sawtooth map with two exits, whose existence is numerically demonstrated in the following way. Let us define

$$W_n^s = \{X | T^t X \notin E \text{ for all } 0 \leq t \leq n\} \tag{7}$$

and

$$W_n^u = \{X | T^{-t} X \notin E \text{ for all } 1 \leq t \leq n\}, \tag{8}$$

where $X = (\theta, J)$ denotes the phase space point, T^t and T^{-t} denote the t th forward and backward images by the map, respectively, and E denotes the union of the exits. In the limit of $n \rightarrow \infty$, the intersection $W_n^s \cap W_n^u$ converges to the invariant set, and W_n^s and W_n^u converge to the stable and unstable manifolds of the invariant set, respectively. Figure 3 shows numerically obtained W_n^s and W_n^u with $n = 15$ and 20 for $w = 0.08$, and it confirms the existence of the homoclinic intersections and the invariant chaotic saddle. It is considered that the fractal part of the basin boundary, i.e., the basin boundary except a small fraction of nonfractal boundary coincides with the closure of the stable manifold of the chaotic saddle, while a segment of the unstable manifold of the chaotic saddle crosses each interior of the two basins.⁹ The existence of the invariant chaotic saddle and the fractal structure of the basin boundary in the system with exits may be interpreted as another manifestation of chaos in the original closed system.

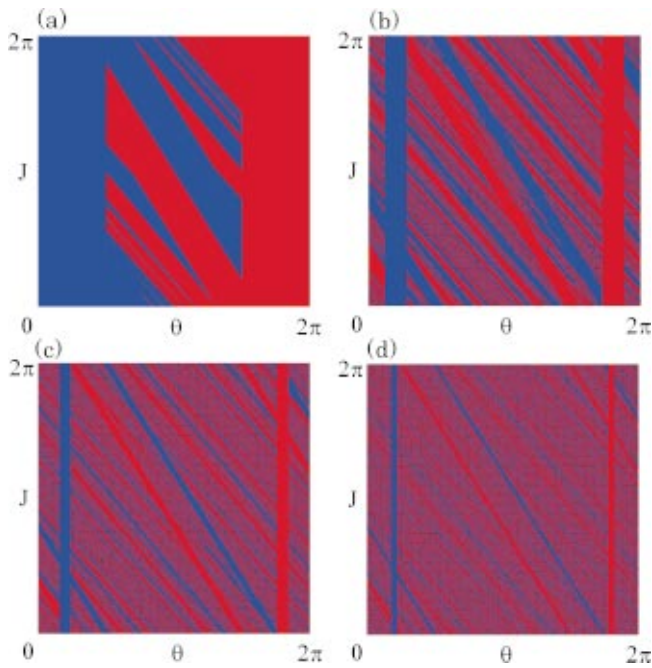


FIG. 1. (Color) Basins of the sawtooth map with symmetrical two exits at $K=0.6$ with (a) $w=0.3$, (b) $w=0.08$, (c) $w=0.04$, and (d) $w=0.02$.

Figure 4 demonstrates the formation process of the chaotic saddle with the decrease of the exit size w . The fact that there is no chaotic saddle in Figs. 4(a)–4(c) contradicting the numerically estimated basin boundary dimension $d \neq 1$ for

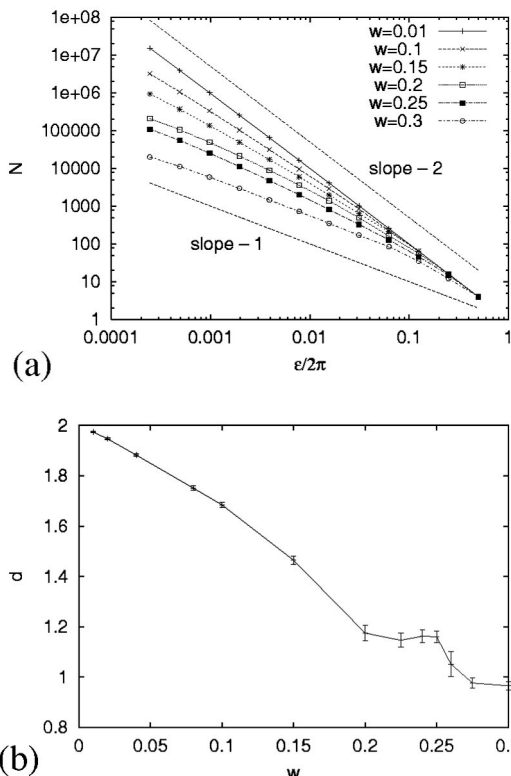


FIG. 2. Basin boundary dimension for the sawtooth map with symmetrical two exits at $K=0.6$: (a) The number N of the uncertain cells against the linear cell size ϵ for several exit sizes. (b) The basin boundary dimension d versus the exit size w estimated for $2^{-12} \leq \epsilon/2\pi \leq 2^{-7}$.

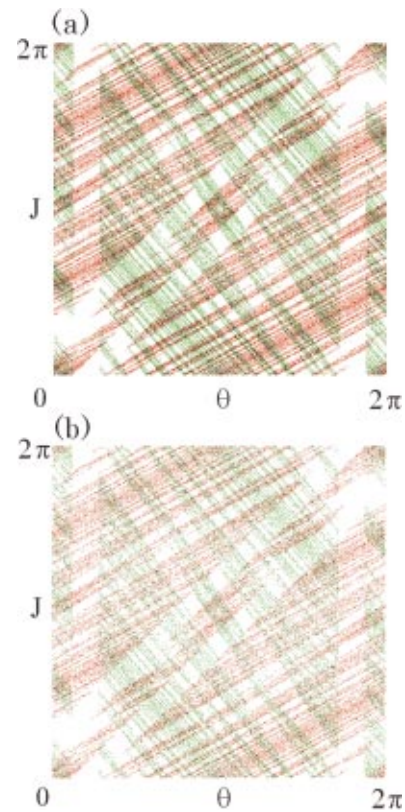


FIG. 3. (Color) W_n^s and W_n^u with (a) $n=15$ and (b) $n=20$ for the sawtooth map with symmetrical two exits of size $w=0.08$ at $K=0.6$. W_n^s , W_n^u , and their intersection are shown in green, red, and black, respectively.

$w \geq 0.2$ in Fig. 2(b) implies that the values of ϵ used for the estimation of d are not sufficiently small.

In the standard map, the last KAM torus breaks up at $K = K_c \approx 0.971\ 635\ 41^{10}$ and the stochasticity of the system is

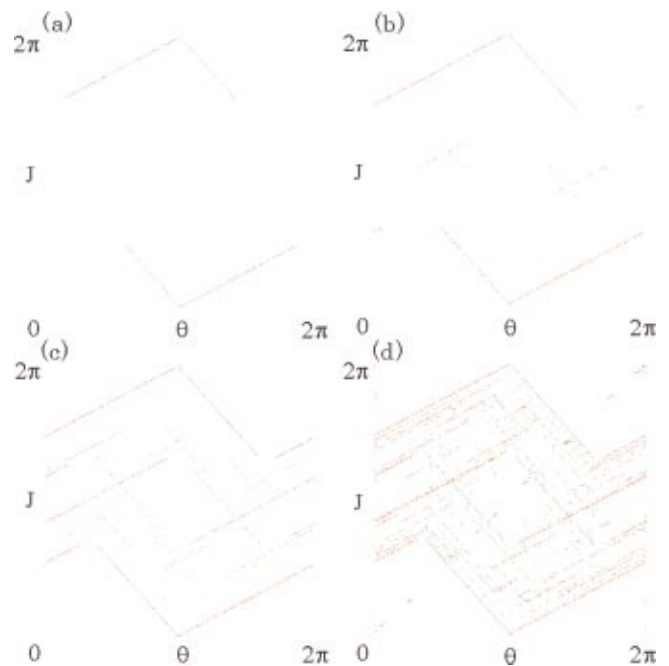


FIG. 4. (Color) W_n^s and W_n^s with $n=10$ for the sawtooth map with symmetrical two exits at $K=0.6$ for the exit size (a) $w=0.3$, (b) $w=0.25$, (c) $w=0.2$, and (d) $w=0.18$.

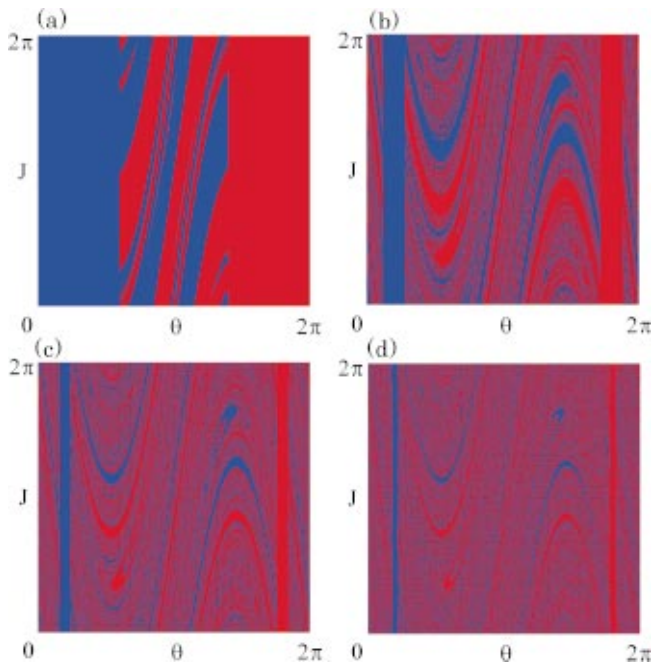


FIG. 5. (Color) Basins of the standard map with symmetrical two exits at $K=8$ with (a) $w=0.3$, (b) $w=0.08$, (c) $w=0.04$, and (d) $w=0.02$.

considered to increase with the increase of value of K . In the following, we denote the accessible region including the unstable fixed point at $(0,0)$ for typical chaotic orbits as the chaotic sea, which has a fat fractal structure¹¹ with holes of resonant island tori.

In Fig. 5, the basins for the standard map with two symmetrical exits at relatively higher value of $K=8$ are shown. In the present resolution 1000×1000 of the phase space, no particular characteristic of nonhyperbolicity is observed but similar fractal basin structure as for the sawtooth map with two exits is observed, i.e., the nonhyperbolic structures such as resonant island tori are small enough and the whole phase space is filled by the chaotic sea at this value of K and the resolution of phase space. In Fig. 6, the basin boundary dimension d is plotted against the exit size w . As in the case of

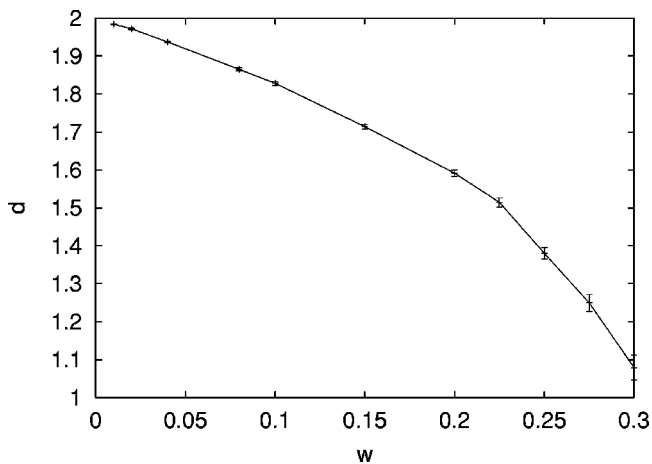


FIG. 6. The basin boundary dimension d versus the exit size w for the standard map with symmetrical two exits at $K=8$.

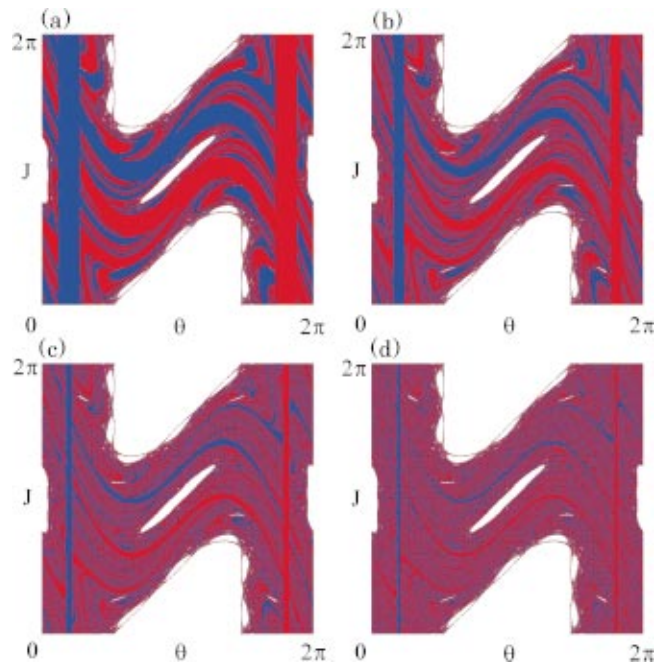


FIG. 7. (Color) Basins of the standard map with symmetrical two exits at $K=2$ with (a) $w=0.08$, (b) $w=0.04$, (c) $w=0.02$, and (d) $w=0.01$.

sawtooth map, the basin boundary dimension d takes a value between 1 and 2 and increases with the decrease of w .

Now let us observe the role of nonhyperbolicity by considering at a relatively small value of K . In Fig. 7, the basins

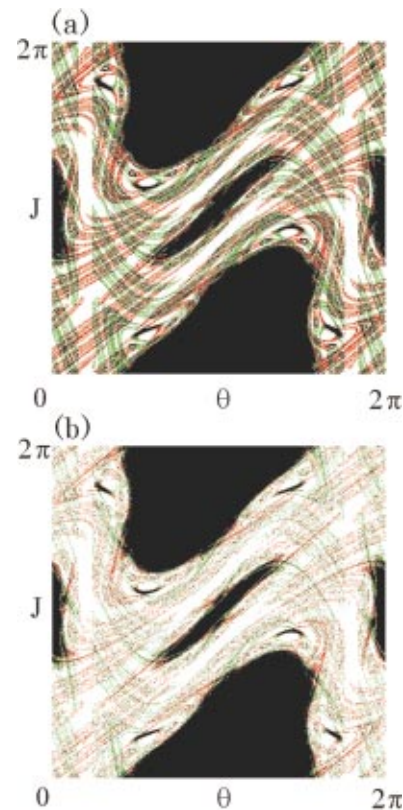


FIG. 8. (Color) W_n^u and W_n^s with (a) $n=20$ and (b) $n=40$ for the standard map with symmetrical two exits at $K=2$ for the exit size $w=0.04$. W_n^s , W_n^u , and their intersection are shown in green, red, and black, respectively. The invariant set is composed of the chaotic saddle and the closed region encircled by island tori.

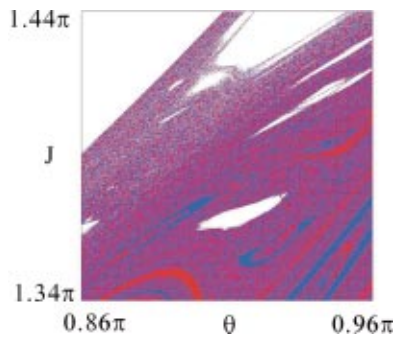


FIG. 9. (Color) Enlargement of a subregion in Fig. 7(b).

for the standard map with two symmetrical exits at $K=2$ are shown, where the blue and red regions show the basins of the left and right exits, respectively. The white region is the set of initial points of orbits, which hit neither of the two exits, and is encircled by critical resonant island tori blocking the chaotic sea. In the middle of the chaotic sea, a similar change of the basin structure for the change of exit size as the case at $K=8$ is observed. As shown in Fig. 8 of W_n^s and W_n^u for $w=0.04$, the chaotic saddle and the resonant island tori compose the invariant set. By comparing the black region, which is the intersection of W_n^s and W_n^u , for $n=20$ and 40 , the slowness of the motion around the critical resonant island tori would be also realized. Figure 9 shows an enlargement of a subregion of Fig. 7(b) around the edge of the chaotic sea. This fractalization of the basin boundary near the critical resonant island tori is due to the fact that it takes a very long time to leave the region near the critical resonant island tori.¹² As shown in Fig. 10 for the system with a larger exit size $w=0.225$, nonfractal basin boundary exists in the middle of the chaotic sea and only the fractalization around the white region is observed. This fractalization implies that

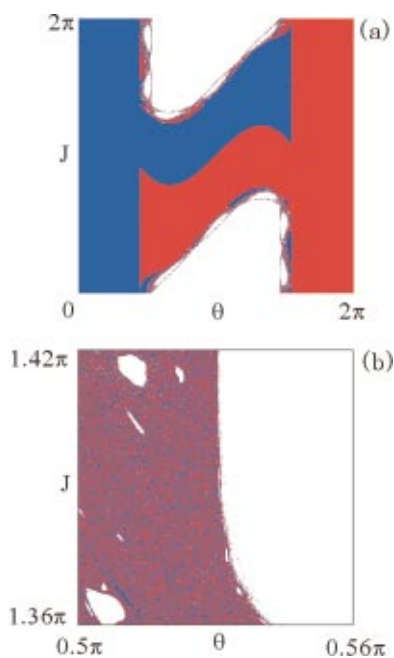
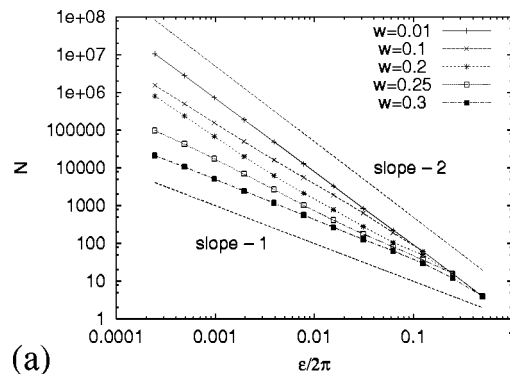
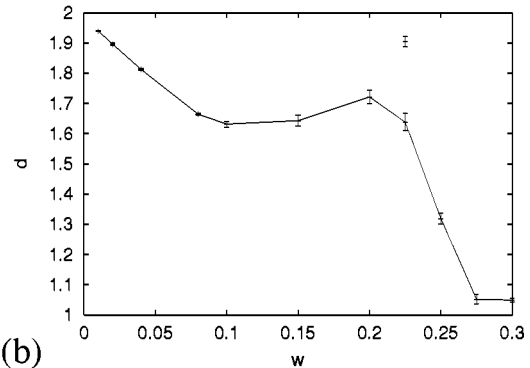


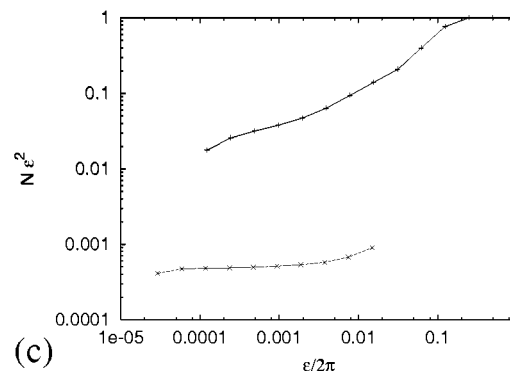
FIG. 10. (Color) (a) Basins of the standard map with symmetrical two exits of size $w=0.225$ and (b) its enlargement of a subregion.



(a)



(b)



(c)

FIG. 11. Basin boundary dimension for the standard map with symmetrical two exits at $K=2$: (a) The number N of the uncertain cells against the linear cell size ϵ for several exit sizes. (b) The basin boundary dimension d versus the exit size w estimated for $2^{-12} \leq \epsilon/2\pi \leq 2^{-7}$. (c) $N\epsilon^2$ versus ϵ for the whole phase space and the subregion shown in Fig. 10(b) at $w=0.225$. The basin boundary estimated from the lower line in (c) is also plotted in (b).

the prediction of the final state is difficult for the initial points close to the white region, while the motion around the white region is relatively regular.

In Fig. 11, the basin boundary dimension is numerically obtained as a function of the exit size w . The basin boundary dimension in Fig. 11(b) shows different behavior from that for the standard map at $K=8$ and the sawtooth map at $K=0.6$ due to the fractalization around the critical resonant island tori. In Fig. 11(c), the number N of uncertain cells over the local region shown in Fig. 10(b) is compared with that over the whole phase space for the system with $w=0.225$ and the corresponding basin boundary dimension d is plotted in Fig. 11(b). It is conjectured that, due to the

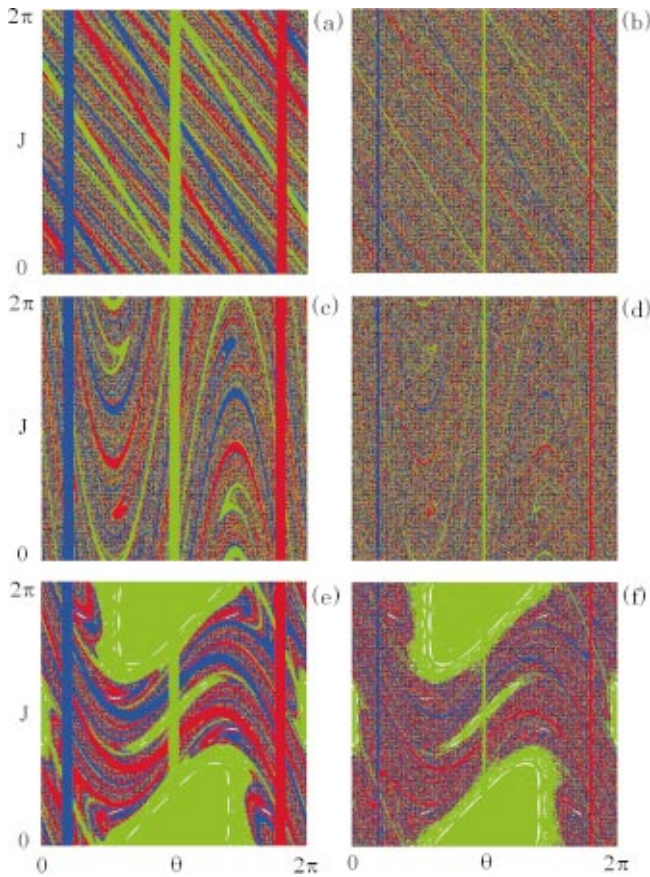


FIG. 12. (Color) Basins for (a), (b) the sawtooth map at $K=0.6$ and (c)–(f) the standard map at (c),(d) $K=8$ and (e),(f) $K=2$ with three exits. The three exits of the same width (a), (c), (e) 0.08π and (b), (d), (f) 0.02π are centered at $\theta=0.2\pi, \pi,$ and 1.8π .

hierarchical structure of cantori around the critical resonant island tori, which is responsible for power law in the residence time distribution, the estimated basin boundary dimension converges to two in the fine limit of the observation.¹³ For large w , the exits cover the resonant island tori and the invariant set becomes to be encircled by a noncritical but regular resonant island torus, which leads to nonfractal basin boundary of $d=1$.

In summary, at $K=2$, we can intuitively state that there are two fractal basin structures due to hyperbolic and nonhyperbolic aspects of the system corresponding to the middle of the chaotic sea and the region around the critical resonant island tori. Around the critical resonant island tori, the nonhyperbolicity has a striking effect on the basin boundary dimension.

B. Wada basins (three exits)

Here let us introduce one more exit. The basins for the system Eq. (3) with three exits are shown in Fig. 12, where the blue, red, and green regions show the basins of the left, right, and center exits, respectively, and the white region is the set of initial points of orbits, which hit neither of the three exits. The basins seem to partly have the Wada property,^{14–16} i.e., the basin boundaries of three basins coincide with each other except a small fraction of nonfractal

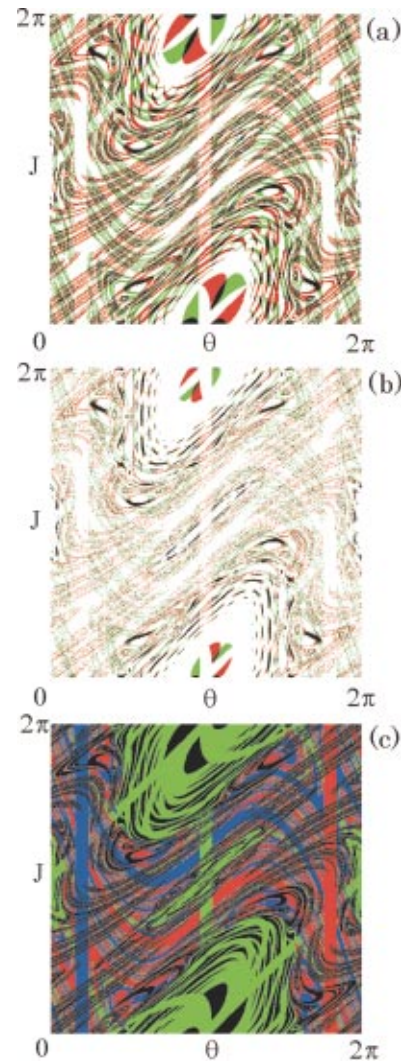


FIG. 13. (Color) W_n^u and W_n^s with (a) $n=15$ and (b) $n=30$ for the standard map with three exits of width 0.08π at $K=2$. $W_n^s, W_n^u,$ and their intersection are shown in green, red, and black, respectively. In (c), W_n^u with $n=15$ is shown in black together with the three basins.

boundary. As in the two exits case, the Wada property of the basin boundaries might be understood by considering the invariant chaotic saddle of the system with three exits, a segment of the unstable manifold of which is believed to cross each interior of the three basins. In Figs. 13(a) and 13(b), W_n^s and W_n^u with $n=15$ and 30 are shown for the standard map at $K=2$. The invariant set is composed of a chaotic saddle and resonant island tori. In Fig. 13(c), W_n^u with $n=15$ is shown in black together with the basins and there seem to be a segment of the unstable manifold which crosses open regions of the three basins.¹⁴

Figures 12(e) and 12(f), for the standard map with three exits at $K=2$, show the case that an exit includes some part of resonant island tori, where the center exit is placed across the largest and second largest resonant island tori. The basin structure over the resonant island tori is almost unchanged with the decrease of the widths of the exits.

An exit of a stripe is generalized to a rectangle by considering the procedure to observe the angle velocity of the rotator besides the angle and stop the rotator if each of the

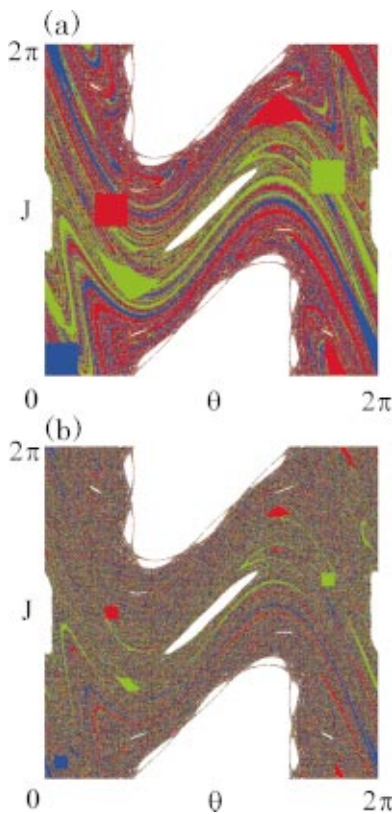


FIG. 14. (Color) Basins for the standard map with three exits of squares at $K=2$. The three squares of the same size (a) $0.2\pi \times 0.2\pi$ and (b) $0.1\pi \times 0.1\pi$ are centered at $(\theta, J) = (0.1\pi, 0.1\pi)$, $(0.4\pi, \pi)$, and $(1.7\pi, 1.2\pi)$.

angles and its velocity is in a given range. In Fig. 14, the basins for the standard map with three exits of squares are shown. The change of basin structure in the chaotic sea with the decrease of exit size is clearly seen. In Fig. 15, the square of exit corresponding the basin shown red in Fig. 14(a) is moved to be included in the resonant island tori. The basin boundary of the red square simply shares with the boundary of the white region.

III. COMPLETE FRACTALIZATION OF PHASE SPACE

As it is observed in Figs. 1, 5, 7, 12, and 14, with the decrease of exit size, the sizes of open balls completely con-

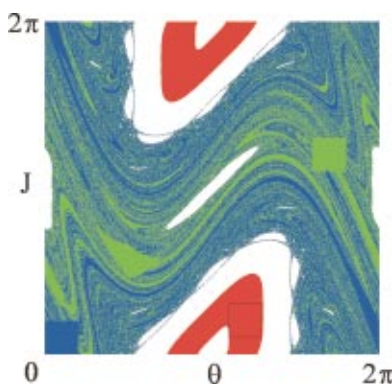


FIG. 15. (Color) Basins for the standard map with the same condition as in Fig. 14(a) except that the exit shown in red is moved to be centered at $(\theta, J) = (1.2\pi, 0.2\pi)$.

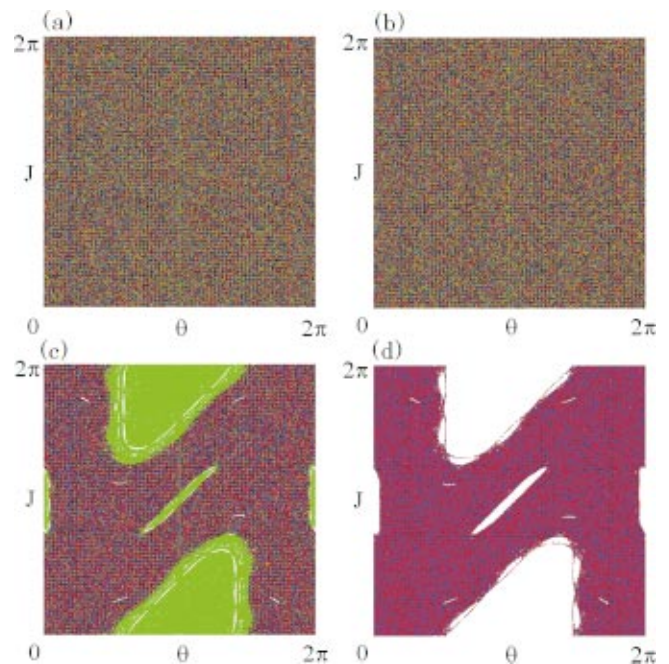


FIG. 16. (Color) Basins for (a) the sawtooth map at $K=0.6$, (b) the standard map at $K=8$, and (c), (d) the standard map at $K=2$ with exits of small size. The three exits are centered at $\theta=0.2\pi$, π , and 1.8π with the same width 0.002π in (a)–(c). The two exits are centered at $\theta=0.2\pi$ and 1.8π with the same width 0.002π in (d).

tained in each of the basins decrease.⁶ In the small size limit of exits, the basin boundary dimension d converges to two and the uncertainty exponent^{1,8} $\alpha = 2 - d$ vanishes, where the error probability to distinguish two different basin points in scale ϵ depends on ϵ as ϵ^α . Figure 16 shows the basins with exits of small size. In the cases of the sawtooth map with three exits at $K=0.6$ and the standard map with three exits at $K=8$, the phase space is almost completely fractalized⁶ as shown in Figs. 16(a) and 16(b), i.e., the points of each basin almost uniformly cover the phase space and the prediction of the final state seems to be very hard. For the standard map with two and three exits at $K=2$, in Figs. 16(c) and 16(d), it is observed that the same is true for the initial points in the chaotic sea.

A similar but different basin structure is known in dissipative systems as the intermingled riddled basins,¹⁷ where the basins contain no open balls. Strictly speaking, in the present system with finite size of exits, the basins contain open balls of which sizes are small but finite. But if the sizes of the exits are small enough compared with the precision of our measurement, then the present unpredictability is stronger than that in the case of intermingled riddled basins due to the fact that the basin points are almost uniformly distributed over the phase space in the present system while they are nonuniformly distributed in the case of intermingled riddled basins, i.e., we can move on the phase space to lower the probability of failure of prediction in the case of intermingled riddled basins.

It should be also noted that the fractalization of the basin boundary around the critical resonant island tori, which leads to $d=2$, for the nonhyperbolic systems with the finite size exits seems to be similar as the intermingled riddled basin.

IV. CONCLUSION

We have demonstrated that when a closed Hamiltonian map is opened, there arise fractal basin boundaries as well as Wada basin boundaries. The basin boundary dimension is numerically obtained as a function of the exit size. The non-hyperbolicity shows a remarkable effect on the basin boundary dimension. It is conjectured that, in the fine limit of the observation, the basin boundary dimension converge to two equivalent to zero uncertainty exponents even for the exit of finite size. In the small size limit of the exits, a complete fractalization of phase space is observed and the deterministic predictability of the final state is almost lost in the chaotic sea. The fractal structure and complete fractalization of the exit basins in the opened system might be considered to be another manifestation of chaos in the original closed system. Let us remark that Hamiltonian maps with exits introduced in the present paper are easily constructed and suitable for numerical investigations. We propose the standard map with exits, as a handy model on open nonhyperbolic Hamiltonian systems, which is useful for the investigation of general properties of open Hamiltonian systems, in particular, concerning the nonhyperbolicity of the systems. For example, a one dimensional lattice of the standard maps with two exits connected through the exits with the nearby maps can be constructed in order to imitate the open Lorentz channel billiard² in a nonhyperbolic way, and the investigation on the relation between the dynamical systems quantity such as the Lyapunov exponents and the Hausdorff dimension and the transport coefficients seems to be an important problem since the nonhyperbolicity introduces a striking effect on the basin boundary dimension as mentioned in Sec. II.

ACKNOWLEDGMENTS

M.A.F.S. acknowledges a short-term program invitation fellowship of the Japan Society for the Promotion of Science for a research stay at the University of Tokyo. This work has been also supported by the Spanish Ministry of Science and Technology under Project No. BFM2000-0967.

- ¹See, e.g., E. Ott, *Chaos in Dynamical Systems* (Cambridge University Press, Cambridge, 1993).
- ²See, e.g., P. Gaspard, *Chaos, Scattering and Statistical Mechanics* (Cambridge University Press, Cambridge, 1998).
- ³See, e.g., papers in *Chaos* **8**(2) (1998).
- ⁴B. V. Chirikov, *Phys. Rep.* **52**, 263 (1979).
- ⁵S. Bleher, C. Grebogi, E. Ott, and R. Brown, *Phys. Rev. A* **38**, 930 (1988).
- ⁶J. Aguirre and M. A. F. Sanjuán, preprint, 2002.
- ⁷I. C. Percival, *AIP Conf. Proc.* **57**, 302 (1979).
- ⁸C. Grebogi, S. W. McDonald, E. Ott, and J. A. Yorke, *Phys. Lett. A* **99**, 415 (1983); S. W. McDonald, C. Grebogi, E. Ott, and J. A. Yorke, *Physica D* **17**, 125 (1985).
- ⁹Due to the existence of homoclinic intersections, the points of the backward images of an open ball across a segment of the unstable manifold, which remain in the interior of the phase space except the exits, might converge to the stable manifold with backward iteration.
- ¹⁰J. M. Greene, *J. Math. Phys.* **20**, 1183 (1979).
- ¹¹D. K. Umberger and J. D. Farmer, *Phys. Rev. Lett.* **55**, 661 (1985).
- ¹²C. F. F. Karney, *Physica D* **8**, 360 (1983).
- ¹³Nonhyperbolic chaotic scattering is investigated in Y. T. Lau, J. M. Finn, and E. Ott, *Phys. Rev. Lett.* **66**, 978 (1991). They conclude that the time delay function is characterized by the uncertainty dimension $d=1$ that corresponds to $d=2$ in our case.
- ¹⁴J. Kennedy and J. A. Yorke, *Physica D* **51**, 213 (1991).
- ¹⁵L. Poon, J. Campos, E. Ott, and C. Grebogi, *Int. J. Bifurcation Chaos Appl. Sci. Eng.* **6**, 251 (1996).
- ¹⁶J. Aguirre, J. C. Vallejo, and M. A. F. Sanjuán, *Phys. Rev. E* **64**, 066208 (2001).
- ¹⁷J. C. Alexander, J. A. Yorke, Z. You, and I. Kan, *Int. J. Bifurcation Chaos Appl. Sci. Eng.* **2**, 795 (1992).